Journal of Machine Engineering, 2026, Vol. 26, No. 1, 93–113
ISSN 1895-7595 (Print) ISSN 2391-8071 (Online)

Received*: 05 November 2025* / Accepted: *16 February 2026* / Published online: *25 February 2026*

plastic gears,
bending fatigue,
tooth-root temperature,
Taguchi–GRA

Trieu The MAI[1,2], Linh Hoang HUYNH[1,2,3],
Loc Huu NGUYEN[1,2*]

TOOTH-ROOT BENDING FATIGUE AND TEMPERATURE ANALYSIS OF PLASTIC GEARS USING THE TAGUCHI–GRA METHOD

This study evaluates and optimizes the tooth-root bending fatigue strength and root temperature of plastic spur gears. It proposes a concise design workflow that couples a Taguchi L18 mixed-level design with grey relational analysis (GRA) and VDI/ISO-based calculations verified by finite-element analysis (FEA). The studied factors include module (m), face-width ratio (b/m), profile shift (x), root fillet radius (ρ/m), normal pressure angle (α), and friction coefficient (μ). Finite Element Analysis (FEA) was employed to determine stress and temperature distributions under realistic loading conditions. An L18 orthogonal array was used for experimental design, and the Grey–Taguchi method enabled multi-objective optimization of conflicting responses. The results show that the module and face-width ratio exert the most significant effects on tooth-root bending stress, whereas the fillet radius strongly influences temperature rise. The proposed Taguchi–GRA approach demonstrates high accuracy with negligible lack of fit, offering a practical and reliable strategy for the design of lightweight and durable plastic gears in machine engineering applications.

1. INTRODUCTION

Gears have long played a vital role in mechanical transmission systems. Historically, they were used in primitive machines. They were then improved to increase lifespan and enhance their ability to work in various conditions. Currently, with the development of the plastics industry, plastic gears are popular due to their amenability to mass-production by injection moulding technology, self-lubrication, and low operating noise [1].

The calculation of tooth-root bending stress has been a significant area of focus for many researchers. Previous literature reveals extensive investigations, including comparative analyses of tooth-root bending strength using different standards and simulations [2]. Other

[1] Faculty of Mechanical Engineering, Ho Chi Minh City University of Technology (HCMUT), Vietnam
[2] Vietnam National University Ho Chi Minh City, Linh Trung Ward, Vietnam
[3] Cao Thang Technical College, Ho Chi Minh City, Vietnam
[*] E-mail: nhloc@hcmut.edu.vn
https://doi.org/10.36897/jme/218159

studies have concentrated on how shape factors and stress concentrations, which are influenced by variations in the tooth-root fillet geometry, affect bending strength [3]. Further research has explored methods for calculating the contact ratio for plastic/plastic and plastic/steel gear pairs [4], evaluated the performance of involute gears concerning bending strength [5], and utilized complex structures for optimization [6]. Furthermore, much of the current research focuses on fatigue. This is also an issue of interest to many authors who reviewed the effects of surface finish on fatigue [7], employed Finite Element Analysis (FEA) software to predict the formation and propagation of fatigue cracks at the tooth-root [8] and compared the influence of different materials using the meshing gear on bending fatigue [9]. Alternatively, from a methodological perspective, the distinction between single-tooth translation testing and multi-tooth rotation testing in bending fatigue evaluation can also be considered [10].

Specifically, for plastic gears, numerous studies have examined the influence of geometric shape on bending strength [11]. Additionally, the thermal behaviour of plastic gears has been a key topic of investigation. For instance, researchers have assessed how different manufacturing methods affect gear quality in relation to operating temperature [12] and compared the operating temperatures of gears made from various materials, such as PA6 and PEI [13]. In addition, for the special type of plastic gear, such as the crossed helical plastic gear, research has been conducted and the methods for predicting the thermal behaviour have been provided [14]. Moreover, geometric modifications [15] and lubrication strategies [16] have been explored as ways to lower the operating temperature of plastic gears. Although many studies on multi-objective optimization of plastic gears have been conducted, they have not yet provided an optimization set of design parameters and bending fatigue curves [17, 18].

Current standards for plastic gears, such as VDI 2736-2 [19], JIS B 1759 [20], and BS-6168 [21], present a notable limitation. They provide generalized bending fatigue curves that are intended for a wide range of design cases. However, any alteration in geometric parameters directly influences the stress distribution, especially at the tooth-root. This localized stress is the primary factor that determines the bending fatigue life of the gear. Consequently, the bending fatigue curve for an optimally designed gear will differ from the standardized curves. Developing a specific fatigue curve that corresponds to an optimal set of parameters would enable designers to select these parameters more effectively and significantly improve the accuracy of plastic gear design. Furthermore, given the inherent temperature sensitivity of plastic materials, another critical objective is to address thermal performance. Therefore, this study will also seek to identify an optimal parameter set that corresponds to the lowest possible temperature generation at the tooth-root during operation.

Following the gear design procedure outlined in VDI 2736-2 [19], the process begins with calculating the tooth-root temperature. However, this initial step, governed by Formula (1), necessitates the determination of the normal module, m_n. The value of m_n is subsequently calculated using Equation (2), a formula that relies on the specified bending fatigue strength of the material.

$$\vartheta_{FuB} \approx \vartheta_0 + P \cdot \mu \cdot H_V \cdot \left(\frac{k_{\vartheta_{FuB}}}{b \cdot z \cdot (v_t \cdot m_n)^{0.75}} + \frac{R_{\lambda,G}}{A_G} \right) \cdot ED^{0.64} \tag{1}$$

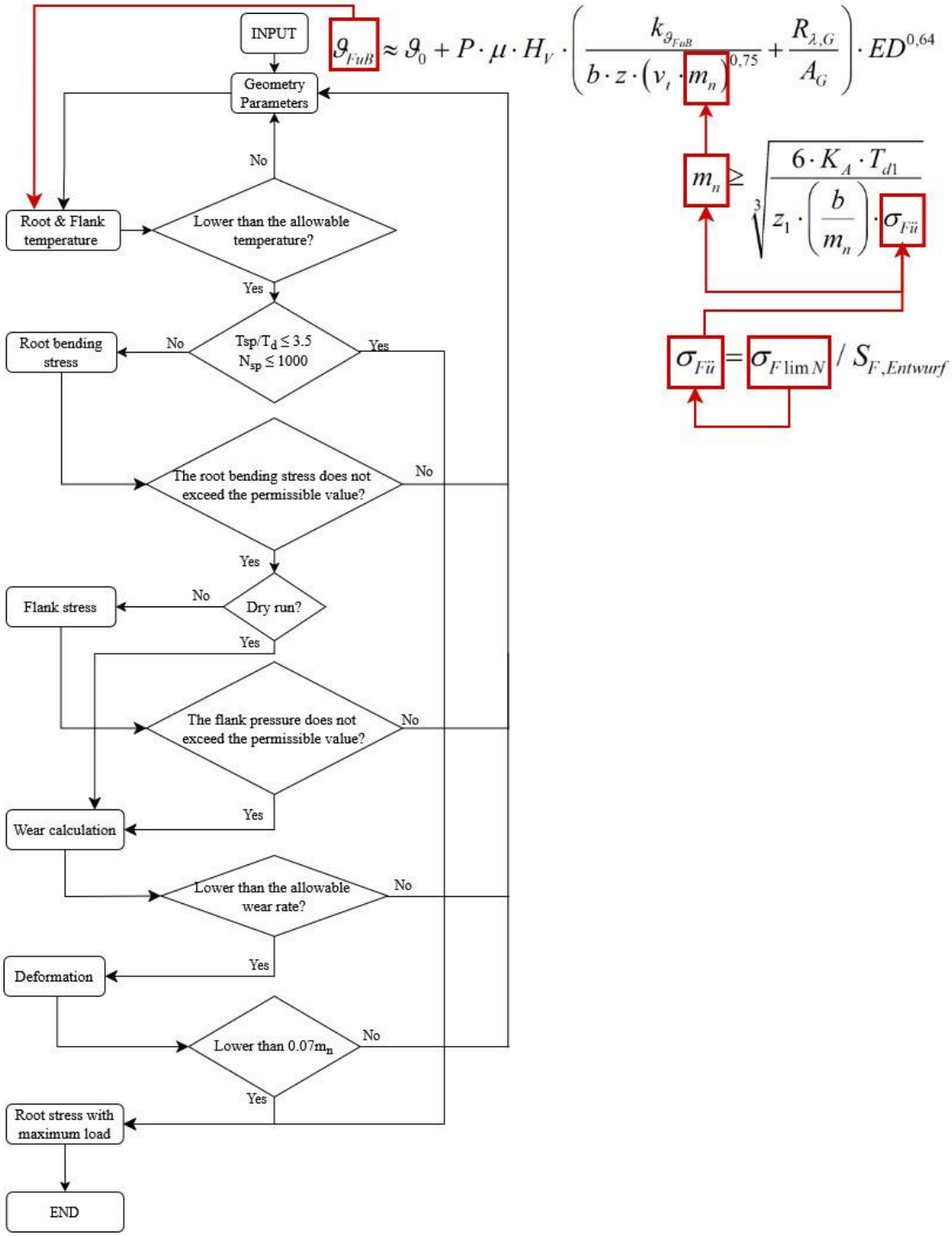

Fig. 1. The influence of bending fatigue strength in the design process according to VDI 2736-2 [19]

$$m_n \geq \sqrt[3]{\frac{6 \cdot K_A \cdot T_{d1}}{z_1 \cdot \left(\frac{b}{m_n}\right) \cdot \sigma_{F\ddot{u}}}} \tag{2}$$

where ϑ_{FuB} is the tooth-root temperature (℃); ϑ_0 is the surrounding temperature (℃); P is the normal power (W); μ is the coefficient of friction; H_V is the tooth loss degree; $k_{\vartheta_{FuB}}$ is

the coefficient of temperature transfer; b is the width of gear (mm); z is the number of teeth; v_t is tangential velocity (m/s); m_n is normal module (mm); $R_{\lambda,G}$ is the resistance of the mechanism housing for heat transfer; ED is relative tooth-engagement time; A_G is the heat-dissipating surface of the mechanism housing (m^2); K_A is the application factor; T_{d1} is nominal torque at the pinion (Nm); $\sigma_{F\ddot{u}}$ is a strength value, $\sigma_{F\ddot{u}} = \sigma_{Flim}/S_F$ (MPa); σ_{Flim} is bending fatigue strength (MPa); S_F is safety factor. This procedural dependence, as illustrated in Figure 1, clearly demonstrates that the bending fatigue strength is a critical input that directly influences the final design parameters and, therefore, the accuracy of the entire design process [19].

Despite significant progress in gear mechanics, the existing literature still exhibits critical limitations in understanding the fatigue behaviors of plastic gears. Most standards continue to rely on generalized S–N fatigue curves, which fail to capture the influence of geometric variations and material-specific responses. Furthermore, the combined effects of bending fatigue strength and tooth-root temperature—two strongly interdependent factors that play a decisive role in gear reliability–have not been systematically investigated.

For these reasons, this study aims to address the above shortcomings through a dual research objective: (i) to evaluate the bending fatigue strength of plastic gears under varying design parameters, and (ii) to analyze the corresponding tooth-root temperature. To achieve this, the Grey–Taguchi method is integrated with numerical simulation in order to identify the optimal set of design parameters. This approach not only minimizes tooth-root stress and temperature simultaneously but also improves the accuracy of gear design procedures, ultimately contributing to more reliable performance predictions for plastic gears.

The novelty and main contributions lie in developing a multi-respond optimization problem for plastic gears, which simultaneously considers both temperature and bending stress to find the optimal parameter set. After determining this optimal set, the corresponding bending fatigue curve is identified and evaluated against the current standard, VDI 2736-2. The remainder of this paper is organized as follows: Section 2 describes the methodology, Section 3 presents the results, and Section 4 provides analysis and discussion.

2. METHODOLOGY

In this study, thermal and mechanical responses are treated sequentially. The tooth-root temperature is calculated from the VDI 2736-2 equations while tabulated parameters and are used as a response in the multi-objective optimization. The mechanical response (tooth-root bending stress) is also evaluated separately using the corresponding VDI 2736-2 bending formulation under the same load and geometry. The temperature result is not used to drive a coupled thermo-mechanical simulation in the present work.

2.1. FACTORS REGARDING BENDING STRENGTH

Although there are currently three calculation standards for plastic gears, namely [19–21], only VDI 2736-2 is truly complete in providing formulas, design procedures, and

the S-N bending fatigue curves. Therefore, this paper will mainly use the formulas from VDI 2736-2. In addition, some factors that need to be analysed in detail will be considered using other standards. The formula of bending stress according to VDI 2736-2 [19]:

$$\sigma_{F\ddot{u}} = K_F \cdot Y_{Fa} \cdot Y_{Sa} \cdot Y_\varepsilon \cdot Y_\beta \cdot \frac{F_t}{b \cdot m_n} \leq \sigma_{FP} \tag{3}$$

where K_F is the factors for tooth-root load with $K_F = K_A \cdot K_v \cdot K_{F\beta} \cdot K_{F\alpha}$; Y_{Fa} is the form factor takes into account the influence of the tooth shape on the nominal bending stress; Y_{Sa} is the stress correction factor; Y_ε is the contact ratio factor; Y_β is the helix angle factor, and because of the spur gear, Y_β = 1; F_t is the nominal tangential force (N); σ_{FP} is permission root stress, $\sigma_{FP} = Y_{St} \cdot \sigma_{FlimN}/S_{Fmin}$ with Y_{St} is the stress correction factor and S_{Fmin} is the minimum safety factor.

Since such factors as K_A, K_v, $K_{F\beta}$ and $K_{F\alpha}$ are not detailed in VDI 2736-2, ISO 6336-3 [22], ISO 6336-1 [23] and [24] are utilized to analyse the final influencing factors. Specifically, the formula and rules mentioned are as follows:

- K_A is the application factor. According to [19] K_A = 1…1.25, in this study, we assume the dynamic effect of the electric motor drive is uniform, so K_A = 1.
- K_v is the internal dynamics factor, which is defined as the ratio of the total mesh torque at operating speed to the mesh torque with a perfect gear. This means that the error of the mesh torque was zero when compared to the quasi-static torque. In this case, it is assumed the error was zero, so K_v = 1 [23].
- $K_{F\beta}$ is related to the effect of the load distribution over the face width on the stress at the tooth-root. This factor can be selected from [24].
- $K_{F\alpha}$ is the traverse load factor for the tooth-root stress regarding the effect of nonuniform distribution of the transverse load, according to [24]:

$$K_{F\alpha} = \frac{4+\left[0.88-3.2\cdot\left(\frac{1}{z_1}+\frac{1}{z_2}\right)\right]\cdot(n_{cx}-5)}{4\cdot\left[1.88-3.2\cdot\left(\frac{1}{z_1}+\frac{1}{z_2}\right)\right]} \tag{4}$$

where n_{cx} is the international tolerance (IT) grades according to ISO 286-1 [25].

In this study, the plastic gears were made by injection molding, and are similar, so n_{cx}= 7 and $z_1 = z_2$. Besides, these coefficients Y_{Fa}, Y_{Sa} and Y_ε also use documents [22–24] to analyze in detail the final influencing factor:

$$Y_{Fa} = \frac{6\frac{h_{Fe}}{m_n}\cdot cos_{aFen}}{\left(\frac{S_{Fn}}{m_n}\right)^2\cdot cos_{an}} \cdot f_e \tag{5}$$

where h_{Fe} is the bending moment arm for tooth-root stress, in this study, is considered the largest value, so h_{Fe}= h = 2.25m [24]; S_{Fn} is the tooth-root chord, in document [22] and S_{Fn} can be calculated similarly to the tooth-root base width in [26] because of the spur gear; f_e is the factors influencing the load distribution between teeth in the mesh, α_{Fen} is the load direction angle [22].

$$Y_{Sa} = \left(1.2 + 0.13\frac{S_{Fn}}{h_{Fe}}\right) \cdot \left(\frac{S_{Fn}}{2\rho}\right)^{\frac{1}{1.21+\frac{2.3}{\frac{S_{Fn}}{h_{Fe}}}}} \quad (6)$$

where ρ is the tooth-root radius.

$$Y_\varepsilon = 0.25 + 0.75/\varepsilon_a \quad (7)$$

where ε_a is the radial contact ratio and ε_1, ε_2 are the partial radial contact ratio of two gears.

Because the two gears are similar [19]:

$$\varepsilon_a = \varepsilon_1 + \varepsilon_2 = 2\varepsilon$$

$$\varepsilon_a = \frac{z}{\pi} \cdot \left(\sqrt{\left(\frac{m \cdot z + 2h_{aP0}}{m \cdot z \cdot cos_a}\right)^2 - 1 - tana}\right)$$

where h_{aP0} is the addendum of the tool standard basic rack tooth profile [26]. In this study, it is considered as $h_{aP0} = h_{aP}$.

2.2 FACTORS RELATED TO TOOTH-ROOT TEMPERATURE

In VDI 2736-2, equation (1) shows that μ, ν_t, and H_V are directly linked to the design variables set of the gear, including [19]:

$$H_V = \frac{\pi(u+1)}{z} \cdot (1 - 2\varepsilon + 2\varepsilon^2)$$

The remaining factors generally do not influence the gear design parameters, but are simply coefficients affected by the transmission. From the analysis in formulas (1) and (3), some final influencing factors can be drawn as displayed in Table 1.

Table 1. Table of factors

Properties	Factors				Tooth-root temperature	Quantity
	$K_{F\beta}$	Y_F	Y_S	Y_ε		
Face width, b	x	x			x	3
Modulus, m		x		x	x	3
Pressure angle, α_n		x		x	x	3
Root fillet radius, ρ			x	x		2
Number of teeth, z				x	x	2
Rotational speed, n					x	1
Friction coefficient, μ					x	1

2.3 OVERALL TAGUCHI–GREY RELATIONAL ANALYSIS (GRA) METHOD

The Taguchi–GRA method is widely recognized as an effective approach for solving multi-objective optimization problems. When combined with the Taguchi experimental

design matrix, it becomes a powerful tool to address multi-objective optimization in experimental planning. An overview of the Taguchi–GRA method can be summarized in the following steps:

1. Design of experiments: Plan and run trials using a Taguchi orthogonal array.
2. Normalization: Normalize each response according to its quality characteristic (larger-the-better, smaller-the-better, or nominal-the-best).
3. Computation: Compute the grey relational coefficients (GRC, ξ) for all responses and their aggregated grey relational grade (GRG).
4. Selection: Identify the factor levels corresponding to the highest GR value.
5. Validation: Re-evaluate the optimization set beyond the Taguchi matrix. If the outcomes are consistent, accept the parameter set as optimal.

3. RESEARCH RESULTS

3.1 GREY-TAGUCHI EXPERIMENTAL MATRIX

In this paper, the research is for gears with power P = 1 kW, material PA66 in a non-lubricated condition; besides the pitch diameter, the rotational speed will be constant to be able to evaluate under the same condition. Because of the spur gear, so the nominal module is replaced by module (m). The factors are selected as follows:

- According to [19], the value of root fillet radius $\rho = 0.25m$. However, this value is obtained according to the reference profile from DIN 867. In addition, when considering the maximum and minimum values that the root fillet radius attains in [27], then $\rho_{max} = 0.5m$ and $\rho_{min} = 0.2m$ so in this paper, the range for $\rho = [0.2; 0.5]m$.

- The value for normal pressure angle α = 14.5°, 20°, 25°, 30° in [24]. The normal pressure angle will affect the tooth-root section. If the normal pressure angle is too small, the tooth-root section will be small as well. This reduces the bending strength, so α = 20°, 25°, 30°.

- According to VDI 2736-2 [19], it is applied to gears with a module greater than 1mm. In addition, in this paper, the gear object is aimed at gears used in power transmission with $m \geq$ 2mm, but the module value should not be too large. In this paper, the maximum module limit is m = 4 mm, so m = 2, 3, 4 mm.

- For the width ratio value b/m, according to VDI 2736-2 [19], in formula (2), to calculate the initial normal module value, it is necessary to select the ratio coefficient b/m, so in fact, the value of b will be identified through selecting the initial ratio coefficient. In [19], the ratio b/m = 5÷20; in this paper the value will be b/m = 8, 12, 16.

- Friction coefficient μ, is in document [19]. Although the material chosen is PA66 for the driving wheel, there are still two cases for transmission designing: PA/PA and PA/steel, at 0.2 and 0.4, respectively. Using a transmission with 2 different components will significantly influence the operating temperature. Therefore, in this paper, both possible design cases are selected. The details are presented in Table 2.

Table 2. Table of factors and levels

N	Factors	Type		Level			Range
		Natural	Code	1	2	3	
1	Ratio of root fillet radius to normal module	ρ/m	x_1	0.2	0.35	0.5	0.15
2	Normal pressure angle, degree	α	x_2	20	25	30	5
3	Module, mm	m	x_3	2	3	4	1
4	Profile shift	x	x_4	0	0.2	0.4	0.2
5	Face width ratio	b/m	x_5	8	12	16	4
6	Coefficient of friction	μ	x_7	0.2	0.4	N/A	0.2

Select constant values: According to VDI 2736-2 [19], the pitch-line (tangential) velocity value provided for PA material is 5 m/s for grease lubrication or dry running cases. Therefore, it is possible to choose the following preliminary values: the tangential velocity is lower than 5 m/s, the rotational speed is 1000 rpm, hence the diameter $d \leq 95.5$ mm, so the diameter d = 84 mm and v_t = 4.7 m/s and torque T = 9.55 Nm are selected.

With 5 factors at 3 value levels, and 1 factor at 2 value levels, the Taguchi L18 mixed experimental design should be used; the details are presented in Table 3.

Table 3. Table of Taguchi L18 and result of experiments

N	Factors												Stress (MPa)	Tooth-root temperature (℃)
	Code						Natural							
	x_1	x_2	x_3	x_4	x_5	x_6	μ	ρ/m	α	m	x	b/m		
1	1	1	1	1	1	1	0.2	0.2	20	2	0	8	27.01	43.94
2	1	1	2	2	2	2	0.2	0.2	25	3	0.2	12	13.77	38.20
3	1	1	3	3	3	3	0.2	0.2	30	4	0.4	16	9.80	35.98
4	1	2	1	1	2	2	0.2	0.35	20	2	0.2	12	21.05	39.29
5	1	2	2	2	3	3	0.2	0.35	25	3	0.4	16	11.73	36.15
6	1	2	3	3	1	1	0.2	0.35	30	4	0	8	7.55	41.97
7	1	3	1	2	1	3	0.2	0.5	20	3	0	16	6.69	37.13
8	1	3	2	3	2	1	0.2	0.5	25	4	0.2	8	8.40	42.79
9	1	3	3	1	3	2	0.2	0.5	30	2	0.4	12	32.66	36.99
10	2	1	1	3	3	2	0.4	0.2	20	4	0.4	12	8.63	49.21
11	2	1	2	1	1	3	0.4	0.2	25	2	0	16	16.01	41.60
12	2	1	3	2	2	1	0.4	0.2	30	3	0.2	8	19.10	52.69
13	2	2	1	2	3	1	0.4	0.35	20	3	0.4	8	17.24	58.50
14	2	2	2	3	1	2	0.4	0.35	25	4	0	12	5.76	47.05
15	2	2	3	1	2	3	0.4	0.35	30	2	0.2	16	18.93	40.48
16	2	3	1	3	2	3	0.4	0.5	20	4	0.2	16	5.13	44.41
17	2	3	2	1	3	1	0.4	0.5	25	2	0.4	8	36.47	53.20
18	2	3	3	2	1	2	0.4	0.5	30	3	0	12	9.55	45.13

3.2. TAGUCHI S/N AND ANOVA ANALYSIS FOR GEAR DESIGN PARAMETERS

Each objective was analyzed independently to quantify the influence of the design parameters. Following the Taguchi methodology, the "smaller-the-better" quality characteristic was applied to both tooth-root stress and temperature. The parameters ρ/m, α, m, and x define the gear geometry and thus are central to the analysis. In contrast, the friction coefficient (μ) exhibits negligible effect on tooth-root stress but is a key determinant of the

temperature response, as referenced by Fig. 2 and 3. Although μ is not governed by geometry, it can still determine design suitability when temperature is the priority criterion (see Fig. 1). In Table 4, For stress, factor x_4 shows the largest contribution (47.1%), followed by x_6 (18.7%) and x_5 (18.6%). The influence ranking is $x_4 > x_6 > x_5 > x_2 > x_3 > x_1$, consistent with the Rank row.

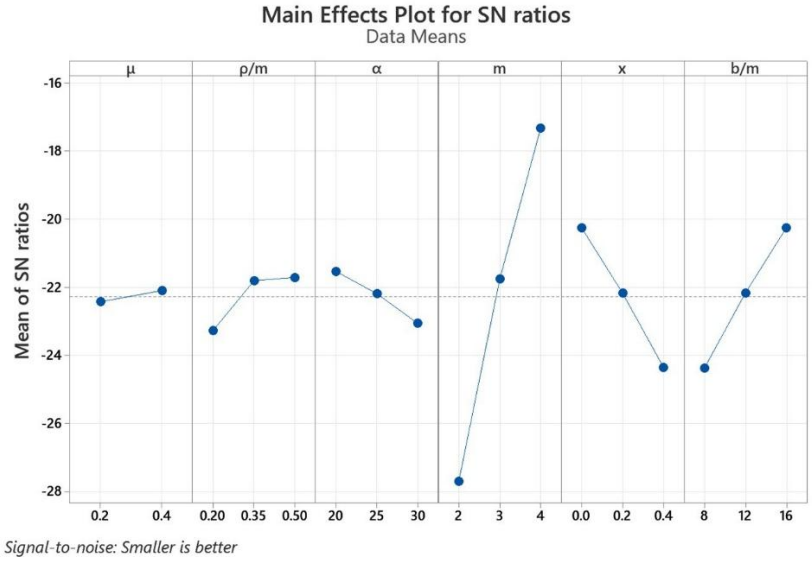

Fig. 2. S/N ratio for stress

Table 4. Response Table for Signal to Noise Ratios of Stress (Smaller is better)

Level	x_1	x_2	x_3	x_4	x_5	x_6
1	-22.44	-23.28	-21.54	-27.71	-20.27	-24.38
2	-22.11	-21.82	-22.20	-21.77	-22.18	-22.18
3	N/A	-21.72	-23.07	-17.33	-24.36	-20.26
Delta	0.33	1.56	1.53	10.37	4.10	4.12
%	1.50	7.09	6.95	47.11	18.62	18.73
Rank	6	4	5	1	3	2

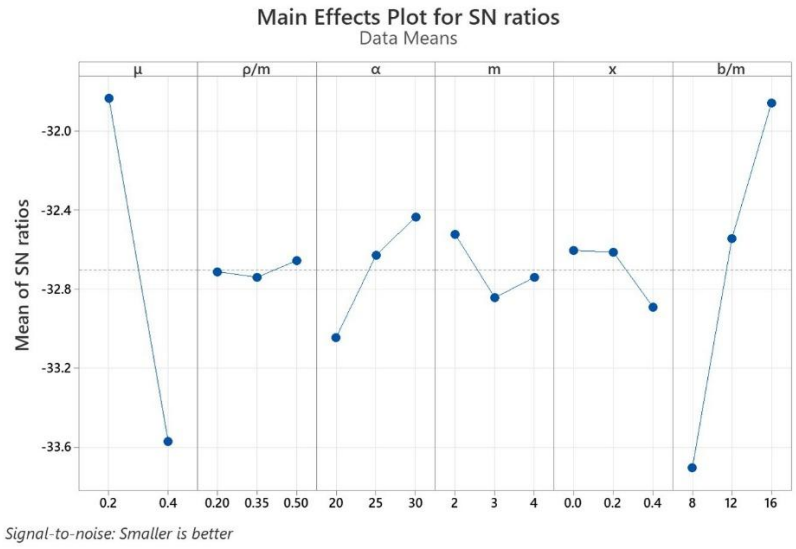

Fig. 3. S/N ratio for temperature

Follow Table 5, the magnitude of influence based on Δ (% contribution): $x_6 \approx 37.8\% > x_1 \approx 35.6\% > x_3 \approx 12.5\% > x_4 \approx 6.5\% > x_5 \approx 5.9\% > x2 \approx 1.6\%$. The dominant factors are x_6 and x_1 (≈73% combined), while x_2 is negligible. Recommended S/N levels: x_1–L1, x_2–L3, x_3–L3, x_4–L1, x_5–L1/2, x_6–L3.

Table 5. Response Table for Signal to Noise Ratios of Temperature (Smaller is better)

Level	x_1	x_2	x_3	x_4	x_5	x_6
1	-31.83	-32.71	-33.05	-32.52	-32.61	-33.71
2	-33.57	-32.74	-32.63	-32.84	-32.61	-32.55
3	N/A	-32.66	-32.44	-32.74	-32.89	-31.86
Delta	1.74	0.08	0.61	0.32	0.29	1.85
%	35.58	1.64	12.47	6.54	5.93	37.83
Rank	2	6	3	4	5	1

ANOVA and statistical interpretation: An L18 orthogonal array was employed to assess six parameters (ρ/m, α, m, x, b/m, μ) for two responses. For stress, m showed the largest S/N range and was significant in ANOVA (α = 0.05), together with b/m and x. For temperature, the 2-level factor μ in a mixed-level array causes overlap, inflating SS and making ANOVA percentages unreliable. A better approach is S/N-based optimization within each μ level.

3.3. TAGUCHI-GRA METHOD

Using the Taguchi–GRA method to find the optimal parameter set with the goal of the stress value being as small as possible:

- Normalize the coefficients with the goal of making them as small as possible:

$$x_i = \frac{\max(y) - y_i}{\max(y) - \min(y)}$$

- Grey relational grade (GRD) and Grey relational coefficient (ξ):

$$\xi_i = \frac{\Delta min + \zeta_{\Delta max}}{\Delta_i + \zeta_{\Delta max}}$$

where Δ_i is the range of differences with $\Delta_i = |x_0 - x_1|$; because normalization x_1 = [0; 1], x_0 = 0, and the smaller-is-better principle, Δ_{min} = 0; $\zeta_{\Delta max}$ is the distinguishing coefficient in the document [28], the authors recommend choosing $\zeta_{\Delta max}$ = [0; 1], and with a balanced distinction and stability of the results, $\zeta_{\Delta max}$ = 0.5.

For the distinguishing coefficient $\zeta_{\Delta max}$, this coefficient has a great influence on the Grey relational coefficient ξ, which will directly lead to the decision to choose the optimal parameter. If $\zeta_{\Delta max}$ is closer to 0, then ξ will have a clear difference when the data changes even very slightly. Consequently, even minor disturbances affect the results. In contrast, if $\zeta_{\Delta max}$ is closer to 1, ξ will reduce the change when there is a disturbance, which will also lose the inherent distinction for the data.

In the theory of Grey [28], the authors also recommend $\zeta_{\Delta max}$ = 0.5. This value is considered the default value [29], at which time the distinction will also be balanced at a moderate level, so as not to be too sensitive to small disturbances and not too blurred by small changes. However, according to research [30], it may not be limited to a specific value, but can be in a range. Also, according to [30], the change in the range of 0.3 to 0.7, the value of ξ approximately remains unchanged. Therefore, in this study, ξ = 0.5 is considered the initial default coefficient for convenience in calculation and selection.

- Since the problem has two output objectives, $GR_{ij} = \frac{\xi_{Si}+\xi_{Ti}}{2}$

where ξ_{Si} is the Grey relational coefficient of stress; ξ_{Ti} the Grey relational coefficient of temperature.

Table 6. Table of normalization, (ξ), and $\overline{GR}$

N	S	x_{Si}	T	x_{Ti}	Δ_{Si}	Δ_{Ti}	ξ_{Si}	ξ_{Ti}	$\overline{GR}$
1	27.01	0.30	43.94	0.65	0.7	0.35	0.42	0.59	0.50
2	13.77	0.72	38.20	0.90	0.06	0.10	0.64	0.84	0.74
3	9.80	0.85	35.98	1.00	0.00	0.00	0.77	1.00	0.89
4	21.05	0.49	39.29	0.85	0.20	0.15	0.50	0.77	0.63
5	11.73	0.79	36.15	0.99	0.03	0.01	0.70	0.99	0.84
6	7.55	0.92	41.97	0.73	0.05	0.27	0.87	0.65	0.76
7	6.69	0.95	37.13	0.95	0.05	0.05	0.91	0.91	0.91
8	8.40	0.90	42.79	0.70	0.00	0.30	0.83	0.62	0.73
9	32.66	0.12	36.99	0.96	0.26	0.04	0.36	0.92	0.64
10	8.63	0.89	49.21	0.41	0.01	0.59	0.82	0.46	0.64
11	16.01	0.65	41.60	0.75	0.40	0.25	0.59	0.67	0.63
12	19.10	0.55	52.69	0.26	0.17	0.74	0.53	0.40	0.47
13	17.24	0.61	58.50	0.00	0.06	1.00	0.56	0.33	0.45
14	5.76	0.98	47.05	0.51	0.03	0.49	0.96	0.50	0.73
15	18.93	0.56	40.48	0.80	0.38	0.20	0.53	0.71	0.62
16	5.13	1.00	44.41	0.63	0.01	0.37	1.00	0.57	0.79
17	36.47	0.00	53.20	0.24	0.39	0.76	0.33	0.40	0.36
18	9.55	0.86	45.13	0.59	0.07	0.41	0.78	0.55	0.67

Table 7. GR coefficient by factors

Factors	Level	GR coefficient
μ	0.2	0.74
	0.4	0.59
ρ/m	0.2	0.64
	0.35	0.67
	0.5	0.68
α	20	0.65
	25	0.6726
	30	0.6723
m	2	0.56
	3	0.68
	4	0.75
x	0	0.70
	0.2	0.66
	0.4	0.64
b/m	8	0.54
	12	0.67
	16	0.78

According to Grey's principle, the result of the calculation is displayed in Table 6, and the factors with the highest Grey coefficient value are selected from Table 7: μ = 0.2; ρ = 0.5m; α = 25; m = 4 mm; x = 0; b/m = 16.

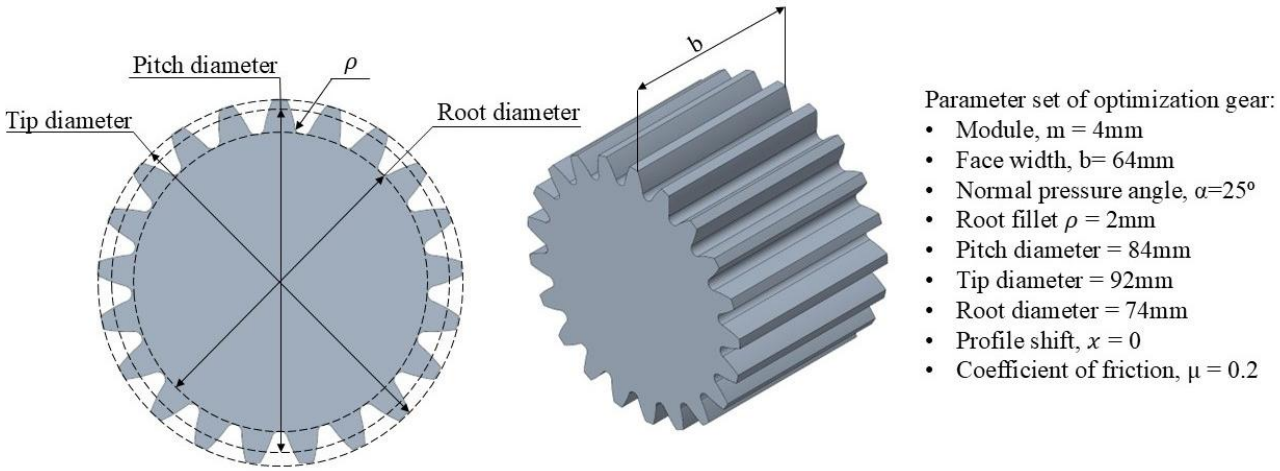

Fig. 4. 3D model of the optimized gear design (optimal parameter set): module m = 4 mm, face width b = 64 mm (b/m = 16), normal pressure angle α = 25°, root fillet radius ρ = 2 mm, pitch diameter d = 84 mm, tip diameter = 92 mm, root diameter = 74 mm, profile shift coefficient x = 0, and coefficient of friction μ = 0.2

If the recently identified parameter set is optimal, then re-evaluating the matrix containing this set should yield the same parameter values. Since the calculation procedure is identical, the results are approximately consistent with those in Table 6, except for the value of N19:

S = 4.52; x_{Si} = 1; T = 36.39; x_{Ti} = 0.98; Δ_{Si} = 0; Δ_{Ti}= 0.02; ξ_{Si} = 1; ξ_{Ti} = 0.96; $\overline{GR}$ = 0.98

Table 8. GR coefficient by factors N19

Factors	Level	GR coefficient
μ	0.2	0.76
	0.4	0.59
ρ/m	0.2	0.64
	0.35	0.67
	0.5	0.72
α	20	0.64
	25	0.71
	30	0.67
m	2	0.56
	3	0.67
	4	0.78
x	0	0.73
	0.2	0.65
	0.4	0.63
b/m	8	0.54
	12	0.67
	16	0.80

From Table 8, the values are those of the N19 parameter set, which still returns the optimal parameter set, meaning the obtained parameter set is suitable. 3D Modeling this parameter set, as displayed in Fig. 4.

Finite element simulations were conducted primarily to verify the stress results obtained from VDI-based calculations rather than to perform a fully coupled thermo-mechanical analysis. The optimized parameter set was evaluated using a single-tooth sector finite element model to reduce computational effort. The predicted tooth-root stress showed good agreement with the analytical calculation according to VDI 2736-2, with a deviation of approximately 0.1%. This agreement supports the analytical–numerical consistency of the optimized design, while experimental validation remains an important subject for future work. The corresponding simulation results are presented in Fig. 5.

In this study, the FEA modeling has been set up in detail:

- Boundary condition: Considering the case of maximum stress, the force should be placed at the tooth edge position, and the constraint is fixed at the hole shaft.
- Element type and mesh size: The major concern in this study was located at the root fillet, and to achieve smoothness and higher accuracy, the element type is quadratic. Based on the mesh convergence study, a locally refined mesh size of 0.02 mm was adopted at the tooth-root fillet. This value falls within the converged range and provides a suitable balance between numerical accuracy and computational cost.
- Material: In this study, we use PA66 with material properties based on [27]. A linear elastic model has been used in this simulation because we are only interested in the maximum stress at the root fillet.
- Convergence: The material behavior is assumed to be linear elastic, resulting in a constant stiffness matrix during the solution process. In addition, the present model does not involve contact interactions or geometric nonlinearity (large deformation). Under these conditions, the numerical solution exhibited stable convergence using the default solver tolerances, and no additional convergence adjustments were required. In addition, a mesh convergence study was performed for the tooth-root region using multiple refinement levels. Local mesh sizes ranging from 0.05 mm to 0.02 mm were considered as fine meshes, while sizes from 1.0 mm to 0.10 mm represented coarser meshes. Based on the convergence assessment, a local mesh size of 0.02 mm was selected as it provides a suitable balance between numerical accuracy and computational cost.

Table 9. Result of simulation convergence data at the tooth-root fillet

Number of elements	Meshing size at tooth-root fillet (mm)		Maximum stress at tooth-root fillet (MPa)
123305	Coarse mesh size	1	4.614
142425		0.5	4.5359
174966		0.3	4.5616
369210		0.1	4.5263
606497	Fine mesh size	0.05	4.5171
903846		0.04	4.517
1392301		0.03	4.5158
3126078		0.02	4.5166

The data in Table 9, Fig. 5b and Fig. 5c indicate that the maximum stress value tended to converge towards a position with a value of approximately 4.52 MPa, so the mesh refinement range from 0.05 mm to 0.02 mm is convergent.

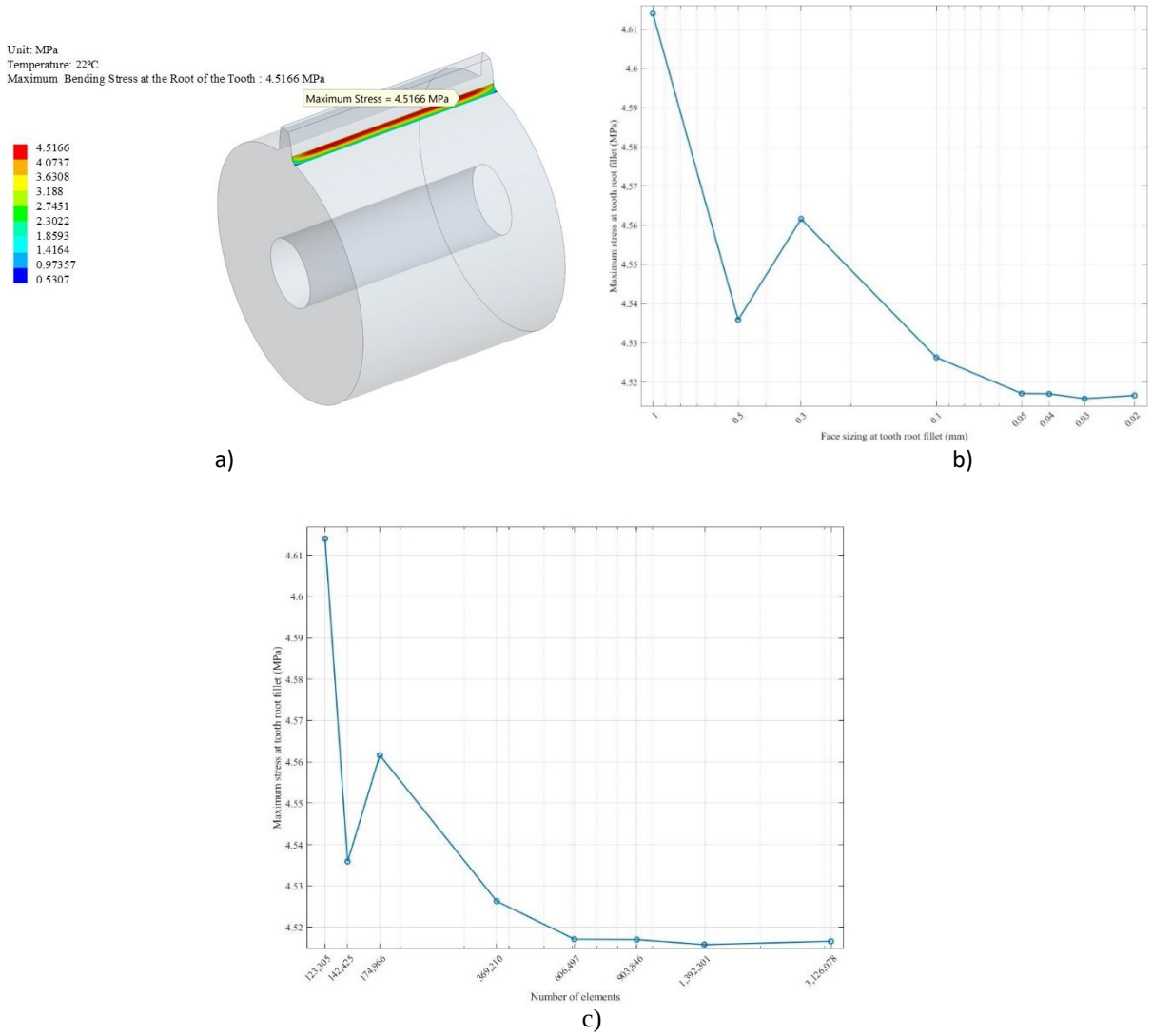

Fig. 5. Finite element simulation results and mesh convergence analysis for the optimized parameter set: (a) maximum bending stress of 4.5166 MPa at the tooth-root fillet; (b,c) mesh refinement and element statistics used for the convergence assessment, showing that the maximum stress stabilizes at approximately 4.52 MPa.

3.4 THE S-N BENDING FATIGUE CURVE

The fatigue curve equation has the form:

$$\sigma_k^m N_k = \sigma_0^n N_0 = const$$

From the perspective of accelerated fatigue testing, determining the fatigue life of gears at low stress levels is often time-consuming due to the large number of failure cycles. In order to shorten the testing time, testing at higher stress levels is applied, thereby quickly

determining the corresponding number of failure cycles. Specifically, by increasing the load up to the maximum level, the gear will quickly reach the failure state in fewer cycles, helping to determine the fatigue limit effectively instead of prolonged testing at low or very small loads.

In addition, in practice, it is not necessary to determine exactly the maximum number of failure cycles corresponding to the lowest stress level. Instead, it is sufficient to determine the lower limit of the load to construct the upper and lower limits of the fatigue curve (S–N curve). According to the study of document [31], the fatigue curve is established by determining the limit regions, including: a high load region corresponding to the lowest number of cycles, a low load region corresponding to the highest number of cycles, and the intermediate region between these two limits, which is the experimental construction region of the fatigue curve.

This paper limits the working range of plastic gears to 10^5 to 10^8 cycles; this choice is based on some existing standards such as VDI-2736, JIS B-1759, and BS-6168. To facilitate the experimental evaluation of fatigue, it is necessary to first conduct simulations on the gears with the optimal parameter set to determine the torque values corresponding to the lowest (10^5) and highest (10^8) number of fatigue cycles. The fatigue curve (S–N curve) used in this study is referenced from the VDI 2736 standard, with PA66 material at 22°C. Due to the limitation from the standard fatigue data, at the highest and lowest cycle numbers, the study only uses one adjacent simulation value; any points outside this range are not considered.

The proposed bending S–N curve in this study is standard/simulation-based, constructed using the VDI 2736-2 fatigue reference, while finite element analysis (FEA) is used only to verify the corresponding stress level for the considered geometry. The curve is therefore intended as a design-point curve for the optimized gear geometry under the assumed operating conditions, and no experimental fatigue validation.

Figure 6 illustrates the data from the simulation in Table 10. Besides, based on VDI 2736-2, when the temperature is constant, the bending fatigue curve for PA66 has the type:

$$S = A + BN^{\frac{1}{n}} \tag{8}$$

Equation (8) can be interpreted using Paris's law in [32] and the fatigue crack of PA6 in [33]:

$$lg(S - A) = lgB + \frac{1}{n} lgN$$

Let $$y = lg\,(S - A),\quad b_0 = lgB,\ b_1 = \frac{1}{n} \text{ and } x = lgN$$

Then: $$y = b_0 + b_1 x \tag{9}$$

For the coefficients A, in this study is selected A =28 for data of simulation in Table 10. Besides, comparing with S-N curve in VDI [19] with the temperature 22ºC as follows:

$$\sigma_{FlimN} = 30 - 0.22 \cdot 22 + (4600 - 900 \cdot 22^{0.3}) \cdot N_L^{\frac{-1}{3}} = 25.16 + 2325.06 \cdot N_L^{\frac{-1}{3}}$$

Therefore, the asymptotic line according to VDI is A = 25.16.

Using the least-squares method in Minitab, we obtain the coefficients of Equation (9) and S-N curve as Table 11. Details of the S-N curve for the two cases are depicted in Figures 7 and 8.

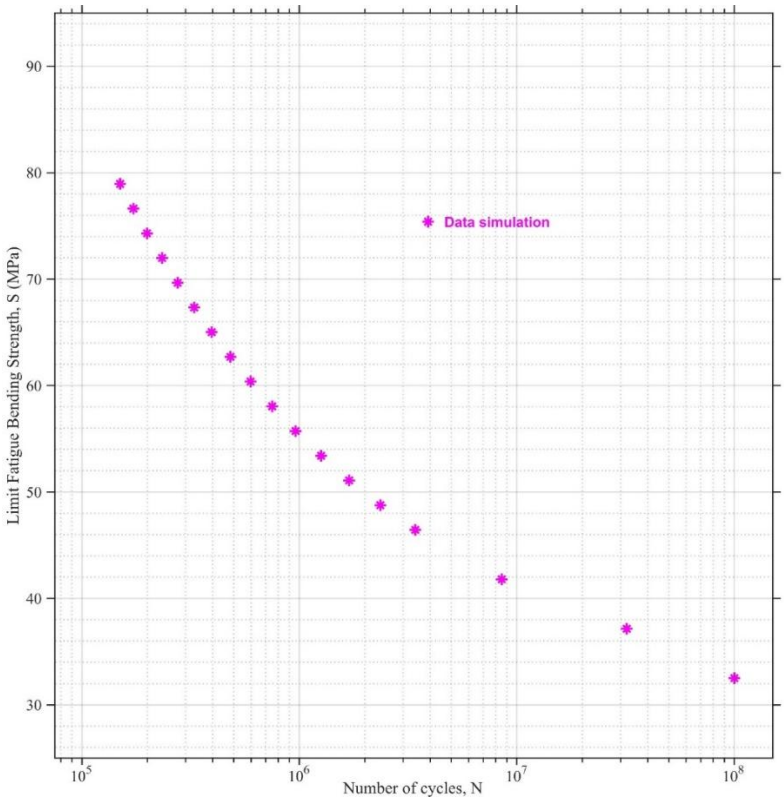

Fig. 6. Chart of simulation data

Table 10. Simulation results for the S–N curve

N	Strength, S, MPa	Number of cycles N	$x = lgN$	$y = \lg(S - A)$ A = 28	$y = \lg(S - A)$ A = 25.16	Fits	Residuals
1	32.51	100000000	8	1.40	0.87	1.7	-0.19
2	37.15	31999000	7.50	1.44	1.08	2.09	0.12
3	41.80	8520000	6.93	1.48	1.22	2.55	0.07
4	46.44	3412200	6.53	1.51	1.33	2.87	0.04
5	48.76	2355800	6.37	1.54	1.37	2.99	0.03
6	51.09	1694000	6.23	1.57	1.41	3.11	0.03
7	53.41	1258800	6.10	1.59	1.45	3.21	0.02
8	55.73	960760	5.98	1.62	1.48	3.31	0.01
9	58.05	749900	5.87	1.64	1.52	3.39	0.01
10	60.38	596250	5.77	1.67	1.55	3.47	0.01
11	62.70	482190	5.68	1.69	1.57	3.54	0.00
12	65.02	395210	5.60	1.71	1.60	3.61	-0.00
13	67.34	328370	5.52	1.73	1.62	3.68	-0.01
14	69.66	275700	5.44	1.40	1.65	3.74	-0.01
15	71.99	233770	5.31	1.44	1.67	3.80	-0.02
16	74.31	199300	5.30	1.48	1.69	3.85	-0.02
17	76.63	172510	5.24	1.51	1.71	3.91	-0.03
18	78.95	149960	5.18	1.54	1.73	3.95	-0.02
19	81.27	130890	5.12	1.57	1.75	4.00	-0.03

Table 11. Results of the S–N equations

A	b_0	b_1	R-sq	Standard error	B	n	S-N
28	3.5119	-0.3467	99.13%	0.0266	$B = 10^{3.5119} = 3250.12$	-2.8843	$S = 28 + 3250.12 \cdot N^{-\frac{1}{2.8843}}$
25.16	3.2503	-0.2943	99.75%	0.0122	$B = 10^{3.2503} = 1779.51$	-3.3979	$S = 25.16 + 1779.51 \cdot N^{-\frac{1}{3.3979}}$

The small standard error of regression S (S = 0.0266) and the high coefficient of determination R-sq (R-sq = 99.13%) indicate that the S–N relationship provides an excellent fit to the experimental data, with no evidence of lack of fit.

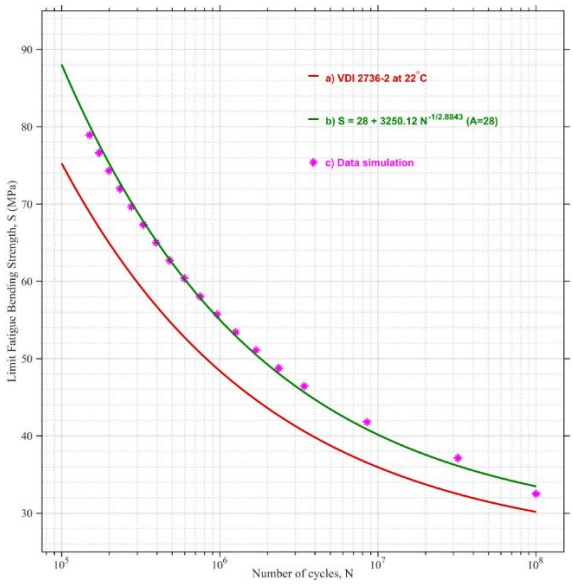

Fig. 7. Bending S–N chart for case A = 28, showing: (a) the VDI 2736-2 reference curve, (b) the regression S–N curve fitted to the simulation data for case A = 28, and (c) the original simulation data points

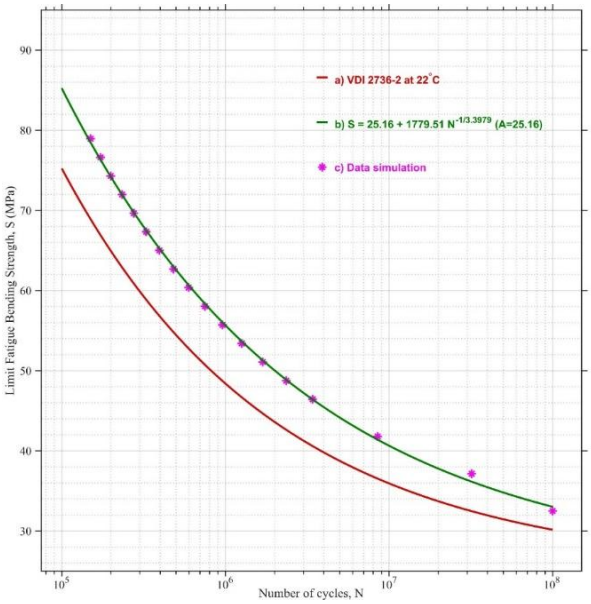

Fig. 8. Bending S–N chart for case A = 25.16, showing: (a) the VDI 2736-2 reference curve, (b) the regression S–N curve fitted to the simulation data for case A = 25.16, and (c) the original simulation data points

4. ANALYSIS AND DISCUSSION

The proposed optimization should be interpreted as a standards-based two-criterion assessment (tooth-root temperature and tooth-root bending stress) at the design-evaluation level. In this sequential workflow, temperature and bending stress are computed from the VDI 2736-2 equations/tables and used as an optimization criterion. Therefore, thermo-mechanical feedback is not included, and the results are intended for consistent ranking of design candidates rather than fully coupled field prediction. This sequential strategy is selected because temperature is used here as a VDI design criterion, while a coupled thermo-mechanical FE model would require reliable temperature-dependent material data and thermal boundary conditions and would substantially increase computational time for the multi-case Taguchi–GRA screening. A fully coupled thermo-mechanical simulation is reserved for future work.

This study addresses the joint reduction of tooth-root bending stress and tooth-root temperature for a polymer gear pair within the VDI 2736–2 framework (with supporting factors from ISO 6336). A Taguchi L18 mixed array was coupled with grey relational analysis to identify robust design settings that do not trade thermal safety for mechanical strength (or vice versa). The screening shows that geometry-driven factors dominate the bending response, whereas the friction coefficient chiefly governs the thermal field at the root.

Factor effects and physical mechanisms: Grey relational grades consistently identify the face-width ratio (b/m) and module (m) as the strongest levers for reducing bending stress. Increasing either of them enlarges the tooth section modulus and thereby lowers nominal root stress. A larger root fillet radius (ρ/m) further diminishes stress by reducing notch severity at the fillet. A zero profile shift (x = 0) avoids thinning at the root. Regarding the normal pressure angle (α), a moderate value (≈ 25°) provides a balanced compromise between tooth thickness and contact ratio (ε). As expected, the friction coefficient (μ) is the primary driver of temperature: lower μ reduces frictional heat input and thus the tooth-root temperature, with negligible direct influence on bending stress. These trends are consistent with classical gear-mechanics arguments and the correction factors embedded in VDI/ISO calculation sequences.

Optimal setting and confirmation test: The Grey-optimal setting is: μ = 0.2, ρ/m = 0.5, α = 25°, m = 4 mm, x = 0, and b/m = 16 (denoted N19). A confirmation run at N19 achieved the highest Grey grade in the augmented matrix and improved both responses simultaneously: tooth-root bending stress = 4.52 MPa and tooth-root temperature = 36.39°C. Compared with the best stress case within the original L18 design (Run 16: 5.13 MPa and 44.41°C), the optimal setting lowers bending stress by approximately 17% and reduces temperature by about 8 °C. The VDI-based calculation and FE simulation agreed within approximately 0.1%, supporting the internal consistency of the analysis pipeline.

Fatigue (S–N) characterization at the optimum: Using the N19 geometry, a bending S–N relation was obtained over $N = 10^5 – 10^8$ cycles. Guided by the constant-temperature assumptions in VDI 2736 and a Paris-law-motivated slope, the regression yields the compact expression:

$$S = 28 + 3250.12 \cdot N^{-\frac{1}{2.8843}} \ (S \text{ in MPa}).$$

This model captures the monotonic increase of allowable stress with decreasing life in the tested range. When compared with the generic PA66 reference at 22°C, the optimized-geometry curve lies predominantly above the reference band. Thus, for a given life, the optimized design sustains higher bending stress, indicating that universal catalog curves can be conservative for well-chosen geometries.

Since the bending S–N curve is standard-/simulation-based, the resulting fatigue-life estimates should be interpreted as comparative design-point predictions rather than an experimentally established material curve for PA66 gears. Deviations may arise from factors not explicitly captured in the present framework, such as material scatter, manufacturing/processing history, and service environment (e.g., temperature and moisture). Experimental validation and calibration (e.g., pulsator or running gear tests) are planned as future work.

Design implications: Geometry first, friction always: prefers larger m, larger b/m, larger ρ/m, and $x \approx 0$ to relieve root stress; then μ should be managed via material pairing or lubrication to control temperature. Moderate α (≈ 25°) provides a practical balance between root thickness and contact ratio; very small or very large angles can harm either strength or load sharing. Integrating temperature early in the sizing loop: co-optimizing thermal and mechanical metrics avoids late-stage iterations and reduces the risk of thermal overload in service.

Limitations and future work: The present study focuses on PA66 at 22°C with discrete friction levels (μ = 0.2 and 0.4) and a fixed speed/power condition. While the Grey–Taguchi approach ranks factor importance and yields a robust setting, it does not replace a full variance decomposition under broad operating envelopes. Unmodeled influences include thermal–mechanical coupling, manufacturing tolerances (e.g., fillet radius scatter, lead/crown errors), moisture and aging effects in polymers, and long-term softening. Future work should expand the environmental and speed/load ranges, include more μ levels and lubrication regimes, and validate the optimized S–N relation via dedicated bending-fatigue tests. Generalization of other polymers (e.g., POM, PBT) and mixed pairs (polymer/steel) is also recommended.

To evaluate the performance of the optimized design in practice, the study proposes a baseline-versus-optimized validation roadmap under the same operating conditions (load, speed, and environment). Representative experimental setups include a bending pulsator (to obtain cycles-to-failure under controlled tooth-root bending) and/or gear test running (to capture service-relevant failure modes). Tooth-root temperature can be monitored using an IR sensor/thermal camera or embedded thermocouples positioned near the tooth-root region, while fatigue performance can be validated through cycles to failure, crack initiation at the tooth-root fillet, and comparison against the VDI-based design criteria. This practical evaluation pathway is identified as future work to validate and calibrate the proposed design-stage framework.

5. CONCLUSIONS

This study identified the optimal parameter set for simultaneously minimizing tooth-root bending stress and temperature in a polymer gear pair, using a combined Taguchi L18 design and grey relational analysis under VDI/ISO-based calculations and FE simulations.

The Grey-optimal setting (μ = 0.2, ρ/m = 0.5, α = 25°, m = 4 mm, x = 0, b/m = 16) reduces root stress by ≈ 17% and temperature by ≈ 8°C. VDI-based and FEA results agree within 0.07%.

Based on this setting, a bending fatigue curve was constructed for PA66 at 22°C: $S = 28 + 3250.12 \cdot N^{-\frac{1}{2.8843}}$ (MPa). This optimized S–N curve lies above the generic reference in VDI 2736-2 across most of the practical life range, indicating that the standard curve may underestimate bending fatigue strength for specific gear geometries and operating conditions.

From a design perspective, the results suggest prioritizing a larger module and face-width ratio, a generous fillet radius, and zero profile shift; adopting a moderate normal pressure angle (α = 25°); and reducing friction through appropriate material selection or lubrication.

Looking forward, extending and validating this methodology across different materials, speeds, loads, and lubrication conditions will help build design-point S–N libraries that complement–rather than replace–the generic curves provided in VDI 2736.

ACKNOWLEDGMENTS

This research is funded by Vietnam National University Ho Chi Minh City (VNU-HCM) under grant number B2024-20-04. We acknowledge Ho Chi Minh City University of Technology (HCMUT), VNU-HCM, for supporting this study.

REFERENCES

[1] GHAZALI W.M., IDRIS D.M.N.D., SOFIAN A.H., SIREGAR J.P., AZIZ I.A.A., 2017, *A Review on Failure Characteristics of Polymer Gear*, MATEC Web Conf. 90, 01029, https://doi.org/10.1051/matecconf/20179001029.

[2] LISLE T.J., SHAW B.A., FRAZER R.C., 2017, *External Spur Gear Root Bending Stress: A Comparison of ISO 6336:2006, AGMA 2101-D04, ANSYS Finite Element Analysis and Strain Gauge Techniques*, Mech. Mach. Theory ,111 ,1–9, https://doi.org/10.1016/j.mechmachtheory.2017.01.006.

[3] LANDI L., STECCONI A., MORETTINI G., CIANETTI F., 2021, *Analytical Procedure for the Optimization of Plastic Gear Tooth-Root*, Mech. Mach. Theory, 166, 104496, https://doi.org/10.1016/j.mechmachtheory.2021.104496.

[4] JABBOUR T., ASMAR G., ABDULWAHAB M., NASR J., 2021, *Real Contact Ratio and Tooth Bending Stress Calculation for Plastic/Plastic and Plastic/Steel Spur Gears*, Mech. Ind., 22, https://doi.org/10.1051/meca/2021029.

[5] ZORKO D., DUHOVNIK J., TAVCAR J., 2021, *Tooth Bending Strength of Gears with a Progressive Curved Path of Contact*, J. Comput. Des. Eng.,8/4, 1037-1058, https://doi.org/10.1093/jcde/qwab031.

[6] NGUYEN L.H., NGUYEN K.T., 2022, *Lightweight Plastic Gear Body Using Gyroid Structure for Additive Manufacturing*, J. Mach. Eng., 22/4, 21–42, https://doi.org/10.36897/jme/157077.

[7] GRZESIK W., 2022, *Influence of Different Machining Processes on Fatigue Life Performance of Engineered Surfaces: A Short Review*, J. Mach. Eng., 22, 2, 18–30, https://doi.org/10.36897/jme/150322.

[8] WANG Z., ZHANG K., SHI L., WANG D., XING H., 2025, *Experimental and Numerical Investigations on Gear Root Crack Propagation Behavior and Fatigue Life*, J. Fail. Anal. Prev., 25/1, 445–457, https://doi.org/10.1007/s11668-025-02119-5.

[9] PANDIAN A.K., GAUTAM S.S., SENTHILVELAN S., 2021, *Effect of Metal and Polymer Mating Gears on the Bending Fatigue Performance of Asymmetric Polymer Gears*, Proc. Inst. Mech. Eng. Part L J. Mater. Des. Appl., 235/10, 2324–2339, https://doi.org/10.1177/14644207211003321.

[10] HONG I., TEAFORD Z., KAHRAMAN A., 2022, *A comparison of gear tooth bending fatigue lives from single tooth bending and rotating gear tests*, Forsch Ingenieurwes, 86, 3, 259–271, https://doi.org/10.1007/s10010-021-00510-w.
[11] HOA V.T., HAO N.P.T., LINH H.H., LOC N.H., 2025, *Research the Influence of the Geometry Parameters to the Bending Strength of the Plastics Gear*, Lecture Notes in Mechanical Engineering, Springer, Cham. 247–253, https://doi.org/10.1007/978-3-031-93816-0_30.
[12] ZORKO D., WEI P., VUKASINOVIC N., 2023, *The Effect of Gear-Manufacturing Quality on the Mechanical and Thermal Responses of a Polymer-Gear Pair*, J. Comput. Des. Eng., 11/1, 195–211, https://doi.org/10.1093/jcde/qwae010.
[13] YILMAZ M., YILMAZ N.F., GUNGOR A., 2024, *Wear and Thermal Coupled Comparative Analysis of Additively Manufactured and Machined Polymer Gears*, Wear, 556–557, 205525, https://doi.org/10.1016/j.wear.2024.205525.
[14] WEBER M., CONSTIEN L., GEITNER M., STAHL K., 2025, *Investigations on the Thermal Behavior of Plastic Crossed Helical Gears*, Forsch. im Ingenieurwes, 89/1, 1–11, https://doi.org/10.1007/s10010-025-00873-4.
[15] SATHEES KUMAR S., SRIDHAR BABU B., PRABHAKAR N., NITHIN CHAKRAVARTHY C., 2021, *Thermal Stress Reduction on Polyamide Gear by Finite Element Method*, Mater. Today Proc., 46, 819–825, https://doi.org/10.1016/j.matpr.2020.12.799.
[16] ILLENBERGER C.M., TOBIE T., STAHL K., 2022, *Operating Behavior and Performance of Oil-Lubricated Plastic Gears*, Forsch, im Ingenieurwes., 86/3, 557–565, https://doi.org/10.1007/s10010-021-00513-7.
[17] TAVCAR J., CERNE B., DUHOVNIK J., ZORKO D., 2021, *A Multicriteria Function for Polymer Gear Design Optimization*, J. Comput. Des. Eng., 8/2, 581–599, https://doi.org/10.1093/jcde/qwaa097.
[18] ELSIEDY M.A., HEGAZI H.A., EL-KASSAS A.M., ZAYED A.A., 2024, *Multi-Objective Design Optimization of Polymer Spur Gears Using a Hybrid Approach*, J. Eng. Appl. Sci., 71/1, 1–17, https://doi.org/10.1186/s44147-024-00443-5.
[19] VDI 2736 BLATT 2, 2014, *Thermoplastic Gear Wheels – Cylindrical Gears – Calculation of the Load-Carrying Capacity*, Engl. VDI-Gesellschaft Produkt- und Prozessgestaltung. Available: https://www.vdi.de/en.
[20] JIS B 1759, 2019, *Estimation of Tooth Bending Strength of Cylindrical Plastic Gears*, Japanese Stand. Assoc. Available: https://webdesk.jsa.or.jp/.
[21] BS 6168:1987, *Specification for non-metallic spur gears*, British Standards Institution (BSI), London.
[22] ISO 6336-3:2019, *Calculation of Load Capacity of Spur and Helical Gears – Part 3: Calculation of Tooth Bending Strength*, Int. Organ. Stand. Available: https://www.iso.org/standard.
[23] ISO 6336-1:2019, *Calculation of Load Capacity of Spur and Helical Gears Part 1: Basic Principles, Introduction and General Influence Factors*, Int. Organ. Stand. Available: https://www.iso.org/standard.
[24] NGUYEN H.L., 2020, *Textbook Fundamental of Machine Design*, Vietnam National University, Ho Chi Minh City, Vietnam (in Vietnamese).
[25] ISO 286-1:2010, *Geometrical Product Specifications (GPS) – ISO Code System for Tolerances on Linear Sizes - Part 1: Basis of Tolerances, Deviations And Fits*, Int. Organ. Stand. Available: https://www.iso.org.
[26] ISO 21771-1:2024, *Cylindrical Involute Gears and Gear Pairs – Part 1: Concepts and Geometry*, Int. Organ. Stand. Available: https://www.iso.org/standard.
[27] RADZEVICH S.P., DUDLEY D.W., 2021, *Dudley's Handbook of Practical Gear Design and Manufacture*, CRC Press, https://doi.org/10.1201/9781003126881.
[28] LIU S., 2025, *Grey Systems Analysis, Series on Grey System*, Springer Nature Singapore, Singapore, https://doi.org/10.1007/978-981-97-8727-2.
[29] AMIN F.A.M., JAAMAN S.H., ROSLAN N.F., 2024, *Analyzing the Impact of Distinguishing Coefficient Parameter in Grey Relational Analysis Model*, AIP Conf. Proc., 3150/1, https://doi.org/10.1063/5.0231308.
[30] MAHMOUDI A., JAVED S.A., LIU S., DENG X., 2020, *Distinguishing Coefficient Driven Sensitivity Analysis of GRA Model for Intelligent Decisions: Application in Project Management*, Technol. Econ. Dev. Econ., 26/3, 621-641, https://doi.org/10.3846/tede.2020.11890.
[31] BONAITI L., GEITNER M., TOBIE T., GORLA C., STAHL K., 2023, *A Comparison Between Two Statistical Methods for Gear Tooth-Root Bending Strength Estimation Starting from Pulsator Data*, Appl. Sci., 13/3, 1546, https://doi.org/10.3390/app13031546.
[32] PARIS P., ERDOGAN F., 1963, *A Critical Analysis of Crack Propagation Laws*, J. Fluids Eng. Trans. ASME, 85/4, 528-533, https://doi.org/10.1115/1.3656900.
[33] ARHANT M., LOLIVE E., BONNEMAINS T., DAVIES P., 2021, *Fatigue Crack Growth Properties of Carbon-Polyamide 6 Thermoplastic Composites Using a Multi-G Control Method*, Eng. Fract. Mech., 252, 107825, https://doi.org/10.1016/j.engfracmech.2021.107825.